equivalent to that of buffer A containing 0.1 M KCl and was applied to a 1-liter phosphocellulose column (P11; Whatman, Maidstone, UK). The column was eluted stepwise at one packed column volume per hour with buffer A containing 0.5 M KCl. Fractions (200 ml) were collected, and active fractions were pooled, adjusted to 1 M $(NH_4)_2SO_4$ by addition of an equal volume of buffer A containing 2 M $(NH_4)_2SO_4$, and applied to a 100 ml Phenyl Sepharose-6 Fast Flow (low sub) column (Pharmacia) equilibrated in buffer D [40 mM Hepes-NaOH (pH 7.9), 0.5 mM EDTA, 1 mM DTT, and 10% (v/v) glycerol] containing 1 M $(NH_4)_2SO_4$. The column was eluted at 10 ml/min with a 1-liter linear gradient from 1 to 0 M $(NH_4)_2SO_4$ in buffer D. Fractions (40 ml) were collected, and the active fractions, which eluted with ~0.6 M $(NH_4)_2SO_4$, were pooled and dialyzed against buffer B [40 mM tris-HCl (pH 7.9), 0.5 mM EDTA, 1 mM DTT, and 10% (v/v) glycerol] to a conductivity equivalent to that of buffer B containing 0.07 M KCl. The dialysate was centrifuged at 20,000*g* for 30 min and applied to a 10-ml Mono-Q column (Pharmacia) equilibrated with buffer B containing 0.07 M KCl. The column was eluted at 1 ml/min with a 100-ml linear gradient from 0.07 to 0.5 M KCl in buffer B. Fractions (4 ml) were collected, and the active fractions, which eluted at ~0.2 M KCl, were pooled, dialyzed against buffer A to a conductivity equivalent to buffer A containing 0.07 M KCl, and applied to a 1-ml Mono-S column (Pharmacia) equilibrated in the same buffer. The column was eluted at 1 ml/min with a 10-ml linear gradient from 0.07 to 0.5 M KCl in buffer A. Fractions (1 ml) were collected, and the active fractions, which eluted with ~0.3 M KCl, were adjusted to 1 M $(NH_4)_2SO_4$ by addition of an equal volume of buffer A containing 2 M $(NH_4)_2SO_4$, centrifuged at 20,000*g* for 30 min, and applied to a Bio-Gel TSK phenyl-5-PW column (7.5 mm by 75 mm; Bio-Rad) equilibrated with buffer D containing 1 M $(NH_4)_2SO_4$. The column was eluted at 1 ml/min with a 30-ml linear gradient from 1.0 M to 0 M $(NH_4)_2SO_4$ in buffer D. Fractions (1 ml) were collected, and the active fractions, which eluted with ~0.5 M $(NH_4)_2SO_4$, were pooled, dialyzed against buffer B to a conductivity equivalent to that of buffer B containing 0.07 M KCl, and applied to a TSK DEAE-NPR (35 mm by 4.6 mm; Toso-Haas, Montgomeryville, PA) equilibrated in the same buffer. The column was eluted at 0.3 ml/min with a linear gradient from 0.07 to 0.5 M KCl in buffer B. Fractions (0.1 ml) were collected, and the active fractions, which eluted with ~0.2 M KCl, were pooled, diluted with an equal volume of 4 M guanidine hydrochloride, 4 M urea, 7.5% acetonitrile, 0.15% trifluoroacetic acid (TFA), and 0.2% Zwittergent ZC-8 (Calbiochem, La Jolla, CA), and applied at 0.1 ml/min to a PLRP-S (1 mm by 50 mm; pore size 1000 Å, particle size 8 μm) rpHPLC column (Michrom BioResources, Auburn, CA) preequilibrated at 40°C in 2% eluant B (90% acetonitrile, 0.09% TFA) and 98% eluant A (2% acetonitrile, 0.1% TFA). The column was developed at 0.1 ml/min with a 2-min linear gradient from 2 to 25% eluant B, followed by a 23-min linear gradient from 25 to 60% eluant B.

7. G. A. Rice, C. M. Kane, M. J. Chamberlin, *Proc. Natl. Acad. Sci. U.S.A.* **88**, 4245 (1991).
8. Pol II (0.01 U) [H. Serizawa, R. C. Conaway, J. W. Conaway, *ibid.* **89**, 7476 (1992)] and 100 ng of pCpGR220 S/P/X (*7*) were incubated at 28°C for 5 min in the presence of 20 mM Hepes-NaOH (pH 7.9), 20 mM tris-HCl (pH 7.9), 2% (w/v) polyvinyl alcohol, bovine serum albumin (0.5 mg/ml), 65 mM KCl, 50 μM $ZnSO_4$, 7 mM $MgCl_2$, 0.2 mM DTT, 3% (v/v) glycerol, 3 U of recombinant RNasin (Promega), 50 μM ATP, 50 μM GTP, 1.8 μM CTP, and 10 μCi of [α-^{32}P]CTP (400 Ci/mmol, Amersham). Transcripts were analyzed by electrophoresis through a 6% polyacrylamide, 7.0 M urea gel.
9. Approximately 50 pmol of PLRP-S–purified rat p80 (*6*) was reduced, *S*-carboxyamidomethylated, digested with trypsin, and fractionated by microbore HPLC. Optimal peptides were determined by differential absorbance of ultraviolet light and matrix-assisted laser desorption mass spectrometry (Lasermat; Finnigan-MAT, San Jose, CA). The peptides were then sequenced by automated Edman degradation [W. S. Lane, A. Galat, M. W. Harding, S. L. Schreiber, *J. Protein Chem.* **10**, 151 (1991)].
10. The human ELL protein was overexpressed in *E. coli* with an M13mpET bacteriophage vector (*20*). The construct for expression of histidine (His)–tagged human ELL was prepared by insertion of a polymerase chain reaction (PCR)–generated 1.8-kb fragment containing the *ELL* ORF into the Sal I and Bam HI sites of M13mpET, which contains the complete pET T7 transcription-translation regions as well as sequences encoding the His tag. The initial *ELL* ORF PCR product encoded a protein with a C494Y mutation relative to the published ELL sequence (*3*). This mutation was corrected by site-directed mutagenesis with the use of the Bio-Rad Muta-Gen kit; the transcription activities of the mutant and corrected proteins were indistinguishable. For preparation of recombinant ELL, a 500-ml culture of *E. coli* strain JM109(DE3) was grown to an absorbance (at 600 nm) of 0.3 with gentle shaking in Luria broth medium containing 2.5 mM $MgCl_2$ at 37°C. Cells were infected with M13mpET carrying the *ELL* ORF at a multiplicity of infection of 20. After 3.5 hours at 37°C, cells were equilibrated at 30°C, induced with 1 mM isopropyl-β-D-thiogalactopyranoside (IPTG), and incubated at 30°C for an additional 12 hours. Cells were harvested by centrifugation at 2000*g* for 15 min at 4°C. Inclusion bodies were solubilized by resuspension in 5 ml of ice-cold 50 mM tris-HCl (pH 8.0) containing 6 M guanidine-HCl, and recombinant His-ELL protein was purified by nickel chromatography on ProBond resin (*20, 21*). For preparation of recombinant ELL protein for transcription assays, 500 ng of His-ELL was renatured essentially as described (*21*). For preparation of SDS-PAGE–purified ELL protein, ~1 μg of His-ELL was subjected to 10% SDS-PAGE. The portion of the gel containing the intact ELL protein was eluted with a Model 422 electroeluter (Bio-Rad). Electroelution was carried out at 10 mA for 4 hours in 25 mM tris base, 192 mM glycine, and 0.1% SDS according to the manufacturer's instructions. The electroeluted His-ELL was ethanol-precipitated and resuspended in 100 μl of 6 M guanidine-HCl, 25 mM tris-HCl (pH 7.9), 300 mM imidazole, and 0.5 mM phenylmethylsulfonyl fluoride. For assays, 20 μl of resuspended His-ELL was diluted with 40 μl of 40 mM Hepes-NaOH (pH 7.9), 0.1 M KCl, 50 μM $ZnSO_4$, 1 mM DTT, and 10% (v/v) glycerol. After 90 min on ice, the protein was dialyzed for 3 hours at 4°C against the same buffer without DTT.
11. A. Shilatifard, R. C. Conaway, J. W. Conaway, unpublished data.
12. P. H. Domer *et al., Proc. Natl. Acad. Sci. U.S.A.* **90**, 7884 (1993).
13. T. Nakamura *et al., ibid.*, p. 4631.
14. R. Prasad *et al., Cancer Res.* **53**, 5624 (1993).
15. O. A. Bernard, M. Mauchauffe, C. Mecucci, H. Van Den Berghe, R. Berger, *Oncogene* **9**, 1039 (1994).
16. J. Corral *et al., Proc. Natl. Acad. Sci. U.S.A.* **90**, 8538 (1993).
17. T. Aso, J. W. Conaway, R. C. Conaway, *FASEB J.* **9**, 1419 (1995).
18. N. F. Marshall and D. H. Price, *J. Biol. Chem.* **270**, 12335 (1995).
19. D. R. Duan *et al., Science* **269**, 1402 (1995); T. Aso, W. S. Lane, J. W. Conaway, R. C. Conaway, *ibid.*, p. 1439; A. Kibel, O. Iliopoulos, J. A. DeCaprio, W. G. Kaelin Jr., *ibid.*, p. 1444.
20. S. Tan, R. C. Conaway, J. W. Conaway, *Biotechniques* **16**, 824 (1994).
21. K. P. Garrett *et al., Proc. Natl. Acad. Sci. U.S.A.* **91**, 5237 (1994).
22. K. P. Garrett *et al., ibid.* **92**, 7172 (1995).

23. We thank R. Robinson of the Harvard Microchemistry Facility for peptide isolation. Supported by NIH grant GM41628 and by funds provided to the Oklahoma Medical Research Foundation by the H. A. and Mary K. Chapman Charitable Trust (A.S., R.C.C., and J.W.C.) and by the William K. Warren Foundation (K.W.J.). A.S. is supported by a postdoctoral fellowship from the Jane Coffin Childs Memorial Fund for Medical Research.

4 January 1996; accepted 23 February 1996

Failure of the Cystic Fibrosis Transmembrane Conductance Regulator to Conduct ATP

M. M. Reddy, P. M. Quinton, C. Haws, J. J. Wine, R. Grygorczyk, J. A. Tabcharani, J. W. Hanrahan, K. L. Gunderson, R. R. Kopito*

The cystic fibrosis transmembrane conductance regulator (CFTR) is a chloride ion channel regulated by protein kinase A and adenosine triphosphate (ATP). Loss of CFTR-mediated chloride ion conductance from the apical plasma membrane of epithelial cells is a primary physiological lesion in cystic fibrosis. CFTR has also been suggested to function as an ATP channel, although the size of the ATP anion is much larger than the estimated size of the CFTR pore. ATP was not conducted through CFTR in intact organs, polarized human lung cell lines, stably transfected mammalian cell lines, or planar lipid bilayers reconstituted with CFTR protein. These findings suggest that ATP permeation through the CFTR is unlikely to contribute to the normal function of CFTR or to the pathogenesis of cystic fibrosis.

The cloning of the CFTR gene (*1, 2*) and the demonstration that it encodes a low-conductance protein kinase A (PKA)–regulated Cl^- channel (*3–5*) confirmed that the loss of epithelial plasma membrane Cl^- conductance is the principal ionic mechanism underlying the pathogenesis of cystic fibrosis (CF) (*6, 7*). The precise mechanism by which this loss of Cl^- conductance is linked to the complex and varied features of the CF phenotype remains obscure. CFTR has been reported to regulate other ion channels (*8, 9*) and mediate permeability of cell membranes to ATP (*10*). Both CFTR (*10*) and its distant relative P-glycoprotein (*11*) have been reported to form ATP-permeant channels with single-channel conductance of ~5 pS. However, we found that CFTR had no detectable ATP conductance in four different systems, including native sweat duct and reconstituted bilayers.

CFTR is abundantly expressed in human sweat duct (*12*), where it appears to constitute the sole pathway for Cl^- absorption (*13*). When the CFTR channel is activated by addition of adenosine 3′,5′-monophos-

phate (cAMP) and ATP to the cytoplasm, the influx of Cl^- causes the luminal side of the apical membrane to become more positive with respect to the cell and the electrical conductance of the membrane to increase. We tested the permeability of ATP through the apical membrane (and therefore through CFTR) by adding 50 mM ATP to a Cl^--free (gluconate substituted) Ringer solution. If ATP is more permeable than gluconate, the luminal side of the membrane should become more positive and its apparent specific conductance should increase. Instead, the apical membrane became slightly more negative (by 6 mV) and the change in specific conductance was negligible (from 2.3 to 3.2 mS/cm^2) (Fig. 1). By contrast, in the presence of a Cl^- gradient, the luminal potential increased by 35 mV and the membrane conductance increased from 9.7 to 14.5 mS/cm^2. The change in transmembrane potential in the presence of ATP was essentially the same as the junction potential for these solutions without the duct present. The slight difference in specific conductance is within experimental error because the specific conductance of the membrane must be calculated from the cable equation (*14*). These results indicate that ATP is not more permeant than gluconate through CFTR in the apical membrane of the sweat duct.

CFTR channels were recorded by the patch-clamp technique in Calu3 cells, a human lung cell line that contains numerous markers indicating that they are a good model for submucosal gland serous cells, including the expression of large amounts of CFTR mRNA, protein, and single-channel currents (*15*). Recordings were made from apical membranes of confluent islands of cells. Whole-cell and short-circuit experiments indicate that CFTR channels are the exclusive Cl^- channels in the apical membranes (*15*). With ATP in the pipette, inward single-channel currents were routinely observed in the cell-attached mode at negative potentials, indicating movement of Cl^- from the cell to the pipette. By contrast, outward single-channel currents through CFTR, indicating ATP movement into the cell, were not observed in seven of seven experiments, even at strong depolarizing potentials (up to +110 mV) (Fig. 2, A and B). Outward currents were observed transiently in three experiments in which the pipette tip was filled with NaCl to facilitate seal formation (Fig. 2C). We interpret the loss of currents in this condition to reflect the gradual replacement of residual Cl^- by ATP in the tip of the electrode because such currents were not observed in the presence of ATP only. The pipette solutions used here are essentially the opposite arrangement from those present in the original experiments reporting ATP conductance (*10*), in which the pipette tip was filled with ATP.

Single-channel and whole-cell currents recorded from Chinese hamster ovary cells stably expressing CFTR also indicate that CFTR does not have measurable conductance to cytoplasmic ATP (Fig. 3). Outward CFTR-mediated single-channel currents were observed in inside-out membrane patches at all positive membrane potentials examined when the pipette solution contained a high concentration of NaCl and the bath contained 100 mM MgATP, as would be expected for Cl^- flow from pipette to bath. By contrast, inward current transitions, corresponding to ATP flow from the bath to the pipette solution, were

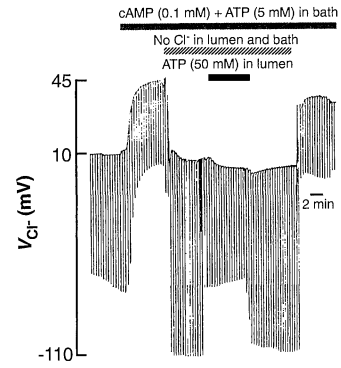

Fig. 1. Lack of ATP permeation in human sweat duct. An isolated segment of a human eccrine sweat duct was microperfused with solutions as indicated by the bars (top) (*22*). The basolateral membrane was functionally removed by selective permeabilization with α-toxin (*23*), after which the cytoplasm was continuously bathed with Cl^--free, K^+ gluconate Ringer solution containing 0.1 mM cAMP and 5 mM ATP in the presence of 1.2 mM Mg^{2+}. Activation of CFTR Cl^- conductance was detected as a rapid increase in luminal potential (lumen relative to bath) and a concomitant increase in membrane conductance indicated by the smaller voltage deflections induced by constant current (50 nA) transepithelial pulses. Cl^- dependence of the potential was shown by replacing Cl^- with the impermeant gluconate anion. The smaller constant current pulse deflections in the presence of 50 mM K^+ ATP occur because ATP substantially reduces the specific resistance of the perfusion solution and thereby the core resistance of the tubule preparation.

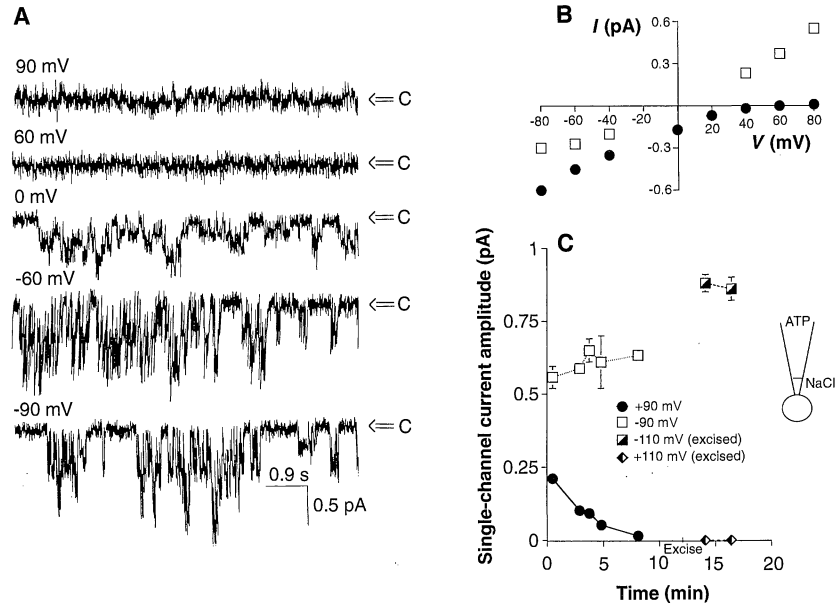

Fig. 2. ATP is not conducted through CFTR channels in the human lung cell line Calu3. (**A**) Single-channel currents through CFTR in cell-attached mode with 100 mM Na_2ATP in the pipette and 150 mM NaCl in the bath. Current records were obtained 8.5 min after seal formation when the Cl^- in the tip had diffused away. Essentially identical results were obtained in five cell-attached patches with 100 mM MgATP and two cell-attached and excised patches with Na_2ATP. All cells were stimulated with 10 μM forskolin. Bath solution contained 150 mM NaCl, 2.5 mM $MgCl_2$, 5 mM KCl, 10 mM Hepes (pH 7.4), 2 mM EGTA, and 0.5 mM ATP. Records were filtered at 100 Hz and sampled at 1 KHz. (**B**) *I-V* relations for four patches with ATP (●, Cl^-/ATP) (n = 4) and six patches with *N*-methyl-D-glucamine Cl^- (□, Cl^-/Cl^-) (n = 6) in the pipette. (**C**) Gradual loss of outward Cl^- current through CFTR channels. The pipette tip was filled with NaCl and the shank was backfilled with Na_2ATP. Points represent the change in absolute single-channel current with time measured at ±90 mV in the cell-attached mode and at ±110 mV after the patch was excised.

M. M. Reddy and P. M. Quinton, Division of Biomedical Sciences, University of California, Riverside, CA 92521, USA.
C. Haws and J. J. Wine, Cystic Fibrosis Research Laboratory, Department of Psychology, Stanford University, Stanford, CA 94305, USA.
R. Grygorczyk, J. A. Tabcharani, J. W. Hanrahan, Department of Physiology, McGill University, Montreal, Quebec, H3G 1Y6, Canada.
K. L. Gunderson and R. R. Kopito, Department of Biological Sciences, Stanford University, Stanford, CA 94305–5020, USA.
*To whom correspondence should be addressed.

not observed under these conditions despite application of large voltages (−110 mV) to drive ATP through the channels (Fig. 3, A and B). No CFTR-mediated ATP currents were observed with 100 mM ATP in both the bath and the pipette, although active CFTR Cl^- channels were observed in the same patches when Cl^- was present on one side of the membrane (*16*). Similar results were obtained when current was measured in the whole-cell configuration with intracellular solution containing 100 mM MgATP and 140 mM NaCl in the bath (Fig. 3, C and D). Leak-corrected whole-cell currents during forskolin stimulation were outwardly rectifying (Fig. 3D) and did not reverse up to at least −110 mV, consistent with single-channel data. This whole-cell membrane current represents inward flow of Cl^- ions from the bath into the pipette. At negative membrane potentials, the inward currents due to outward flow of ATP anions or inward flow of cations (or both) from the bath through CFTR and other channels were negligible under these conditions and provide further evidence that CFTR does not mediate ATP conductance.

Finally, ATP permeation through CFTR was examined in artificial planar lipid bilayers reconstituted with recombinant CFTR (Fig. 4). Reconstitution of wild-type CFTR into planar bilayers in 300 mM KCl revealed small (9 to 10 pS), ATP-dependent Cl^- channels that exhibited the characteristic slow gating pattern of CFTR (*17, 18*). The orientation of these channels upon fusion into the bilayer is such that the cytoplasmic side of CFTR faces the cis chamber (*17*). Exchange of the cis solution with a Cl^--free solution containing 100 mM Na_2ATP abolished all conductance at negative (cis to trans) potentials (Fig. 4). The current-voltage (*I/V*) relation of CFTR channels with 100 mM ATP (cis) and 300 mM KCl (trans) revealed Cl^--conductive channels at positive potentials, the amplitude of which gradually decreased to zero as the potential was reduced to −80 mV. Addition of 300 mM KCl (in addition to the 100 mM ATP) to the cis chamber restored the linear *I/V* relation, with a slope conductance of 8.9 pS. Similarly, when the ATP gradient was reversed (that is, 100 mM Na_2ATP trans and 300 mM KCl cis), currents were detected only at negative potentials, consistent with Cl^- permeation, but not at positive potentials up to +100 mV, confirming that ATP does not permeate the channel. Finally, no currents were detected when both cis and trans chambers contained 100 mM ATP as the sole anion (*19*). These data therefore demonstrate that functional CFTR channels reconstituted into planar bilayers fail to reveal conductance to ATP.

Our results demonstrate that ATP is not conducted through CFTR in intact organs, polarized human lung cell lines, stably transfected mammalian cell lines, or planar lipid bilayers reconstituted with recombinant CFTR. This lack of permeability to ATP is fully compatible with estimates of the pore diameter of CFTR (≤5.5 Å) (*20*) and the smallest silhouette dimensions for ATP (10.5 Å) (*21*). The currents originally interpreted as being mediated by ATP flow through CFTR channels had variable amplitudes, kinetic properties, and responses to blockers (*10*) and might therefore represent some combination of currents carried through CFTR by ions other than ATP or ATP currents through channels or permeation pathways other than CFTR. It is possible that such alternative pathways for ATP permeation are related to CFTR expression, but the relation is apparently not obligatory.

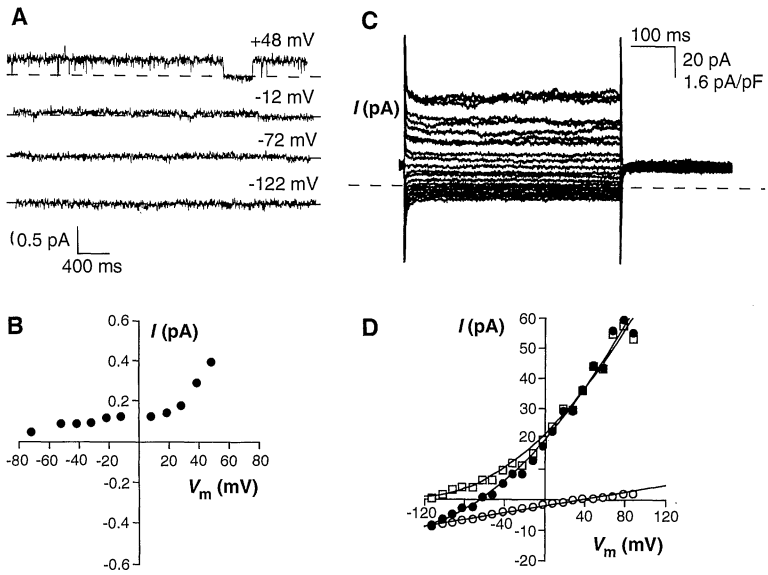

Fig. 3. Effect of high intracellular ATP on single CFTR channel and whole-cell currents. (**A**) Excised inside-out patch recordings with bath solution containing 100 mM MgATP (Sigma), 75 nM PKA (Promega), and 10 mM *N*-tris[hydroxymethyl]methyl-2-aminoethane-sulfonic acid (TES) (pH 7.4). The pipette solution contained 150 mM NaCl, 2 mM $MgCl_2$, and 10 mM TES (pH 7.4). (**B**) Single-channel *I-V* relation with 100 mM ATP bathing the cytoplasmic side. (**C**) Whole-cell current measured with the same 100 mM MgATP solution in the pipette and with bath solutions containing 140 mM NaCl, 5 mM KCl, 1.2 mM $CaCl_2$, 1.2 mM $MgCl_2$, 10 mM TES (pH 7.4), and 10 μM forskolin. Broken line indicates zero current. (**D**) *I-V* relations during the same experiment shown in (C). Pipette currents were measured in the cell-attached configuration (○) and 150 s after breaking into the whole-cell configuration by applying excess suction (●). The leak-corrected current flowing through the cell membrane (□) was approximated as the difference between the total current after breaking into the cell minus the current flowing through the seal between the cell membrane and glass pipette in the cell-attached configuration (*24*).

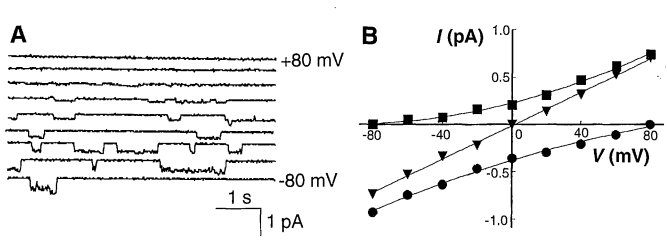

Fig. 4. Failure of CFTR to mediate ATP conductance when reconstituted into planar lipid bilayers. (**A**) Single-channel records of CFTR expressed in human embryonic kidney (HEK) cells and reconstituted into a planar lipid bilayer prepared as described (*17, 18*), held at different potentials from −80 to 80 mV (cis side of bilayer with respect to trans) in 20-mV increments. The ionic conditions were 300 mM KCl (pH 7.2) (cis) and 100 mM Na_2ATP (pH 7.2) (trans). The Cl^- solution contained 10 mM MOPS, 1 mM Na_2ATP, and 1 mM $MgCl_2$. The ATP solution contained 10 mM MOPS and 1 mM $MgCl_2$. (**B**) *I-V* relations for CFTR channels under three different cis:trans ionic conditions: 300 mM KCl:100 mM Na_2ATP (●), data from the traces shown in (A); 100 mM Na_2ATP:300 mM KCl (■); and 100 mM Na_2ATP supplemented with 300 mM KCl:300 mM KCl (▼). The latter conditions yielded a linear *I-V* relation corresponding to a single-channel conductance of 8.9 pS.

REFERENCES AND NOTES

1. J. M. Rommens *et al.*, *Science* **245**, 1059 (1989).
2. J. R. Riordan *et al.*, *ibid.*, p. 1066 (1989).
3. N. Kartner *et al.*, *Cell* **64**, 681 (1991).
4. M. P. Anderson *et al.*, *Science* **253**, 202 (1991).
5. C. E. Bear *et al.*, *Cell* **68**, 809 (1992).
6. P. M. Quinton, *Nature* **301**, 421 (1983).
7. _____, in *Fluid and Electrolyte Abnormalities in Exocrine Glands in Cystic Fibrosis*, P. M. Quinton, J. R. Martinez, U. Hopfer, Eds. (San Francisco Press, San Francisco, CA, 1982), pp. 53–76.
8. E. M. Schwiebert *et al.*, *Cell* **81**, 1063 (1995).
9. M. J. Stutts *et al.*, *Science* **269**, 847 (1995).
10. I. L. Reisin *et al.*, *J. Biol. Chem.* **269**, 20584 (1994).
11. E. H. Abraham *et al.*, *Proc. Natl. Acad. Sci. U.S.A.* **90**, 312 (1993).
12. N. Kartner, O. Augustinas, T. J. Jensen, A. L. Nai-

smith, J. R. Riordan, *Nat. Genet.* **1**, 321 (1992).
13. M. M. Reddy and P. M. Quinton, *Am. J. Physiol.* **267**, C1136 (1994).
14. R. Greger, *Pflueg. Arch. Eur. J. Physiol.* **390**, 30 (1981).
15. C. Haws, W. E. Finkbeiner, J. H. Widdicombe, J. J. Wine, *Am. J. Physiol.* **266**, L502 (1994); B. Q. Shen, W. E. Finkbeiner, J. J. Wine, R. J. Mrsny, J. H. Widdicombe, *ibid.*, p. L493.
16. R. Grygorczyk, J. A. Tabcharani, J. W. Hanrahan, *J. Membr. Biol.*, in press.
17. K. L. Gunderson and R. R. Kopito, *J. Biol. Chem.* **269**, 19349 (1994).
18. ———, *Cell* **82**, 231 (1995).
19. ———, unpublished data.
20. J. W. Hanrahan, J. A. Tabcharani, R. Grygorczyk, in *Cystic Fibrosis, Current Topics*, J. A. Dodge, D. J. H. Brock, J. H. Widdicombe, Eds. (Wiley, Toronto, 1993), pp. 93–137.
21. H. B. Bull, *An Introduction to Physical Biochemistry* (Davis, Philadelphia, 1972).
22. Sweat glands were obtained by skin punch biopsy from healthy volunteers who gave informed consent. Segments (1 to 2 mm in length) of reabsorptive ducts were microdissected from single sweat glands and microperfused as described (*13*). To reduce the duct preparation to a single membrane with Cl^- conductance only, all luminal perfusion solutions contained 140 mM K^+ (no Na^+) and 10 to 5 mM amiloride to remove any Na^+ conductance. Cl^-, gluconate, and ATP were substituted as required. The cytoplasmic bath solution contained 140 mM K^+ gluconate with 10^{-4} M cAMP and 5 mM ATP added as required. All solutions contained 1 mM $CaCl_2$, 1.2 mM $MgSO_4$, 2 mM K_2EGTA, and 3 mM K_2HPO_4 (pH 7.3). Measurements were made at 35° ± 2°C. Constant current pulses of 50 nA and 0.5-s duration were applied through one barrel of a double cannula perfusion pipette. Luminal perfusates were introduced, and luminal potentials were measured through the other barrel.
23. P. M. Quinton and M. M. Reddy, *Nature* **360**, 79 (1992).
24. Standard single-channel and whole-cell patch-clamp methods were used [O. P. Hamill, A. Marty, E. Neher, B. Sakmann, F. J. Sigworth, *Pflueg. Arch. Eur. J. Physiol.* **391**, 85 (1981)]. In whole-cell experiments, 500-ms voltage steps of −112 to +88 mV were applied in 10-mV increments every 2 s from the holding level of 0 mV. The pClamp 6 software and TL-1 DMA interface (Axon Instruments) were used to generate the command potentials and for data acquisition. When the pipette or bath (or both) contained ATP, electrical connection to the Ag-AgCl electrode was made through an agar bridge containing NaCl solution. Liquid junction potentials were measured against a flowing 3 M KCl electrode [E. Neher, *Methods Enzymol.* **207**, 123 (1992)]. All voltages shown were corrected for liquid junction potentials.
25. We thank S.-X. Zheng and J. Liao for technical assistance. Supported by grants from the National Institutes of Health (DK43994 to R.R.K., HL42368 and DK45913 to J.J.W., and DK41329 to P.M.Q.), the Canadian and U.S. Cystic Fibrosis Foundations, the Medical Research Council (Canada), Cystic Fibrosis Research, Inc., and gifts from Patricia Bresee and Kay and Ronald Presnell. This work was done during the tenure of an Established Investigatorship of the American Heart Association (R.R.K.), a U.S. Cystic Fibrosis Foundation postdoctoral followship (K.L.G.), and a Medical Research Council Scientist award (J.W.H.).

6 November 1995; accepted 22 January 1996

TECHNICAL COMMENTS

Testing for Bias in the Climate Record

We have tested two of the conclusions made by David J. Thomson in his article (*1*): That "anomaly series in climate research that have been deseasonalized by subtracting monthly averages need to be recomputed" and that "significant efforts must be made to understand the consequences of the annual temperature cycle following precession rather than the equinoxes, and of the capture effect." Unlike Thomson, we used daily data, which is necessary to detect possible bias resulting from precession in an instrumental climate record based on deseasonalized climate trends.

We tested Thomson's assertions with the use of 144 long-term stations (each station generally spanning about 75 to 85 years) within the contiguous United States. Most of these stations were derived from the U.S. Historical Climate Network (*2*). We also used the longest homogeneous daily series available, the Central England Temperature (CET) time series (*3*). Using these series, we estimated the change in monthly, seasonal, and annual trends, allowing for the change in perihelion dates. Over the span of the CET time series, 219 years, the change is about 5 days, and for the U.S. stations the change amounts to 2 days (perihelion shifts toward increasing Julian days). We compared monthly trends of temperature (calculated from deseasonalized anomalies of daily mean, maximum, and minimum temperatures based on Gregorian calendar months) with trends derived from deseasonalized values [where the days included in each month were offset by the change in the date of perihelion from the beginning of the record to the end of the record (*4*)]. Such a test bounds the maximum impact of precession because the differences will also result from seasonal effects and the random effects of weather as well as any effects due to precession of the orbit.

We found that incorporating perihelion calendar shifts in the network of U.S. stations had no effect on the annual mean temperature trends. However, monthly differences did appear (Fig. 1), but a question arose with regard to the significance of the monthly difference. How much is simply due to random chance (that is, the vagaries of weather over two days during the course of 75 to 85 years)? This may be reflected by the end of 1 month having a spell of weather significantly different from the beginning of the next month. Even over long records it is conceivable that such an effect may not

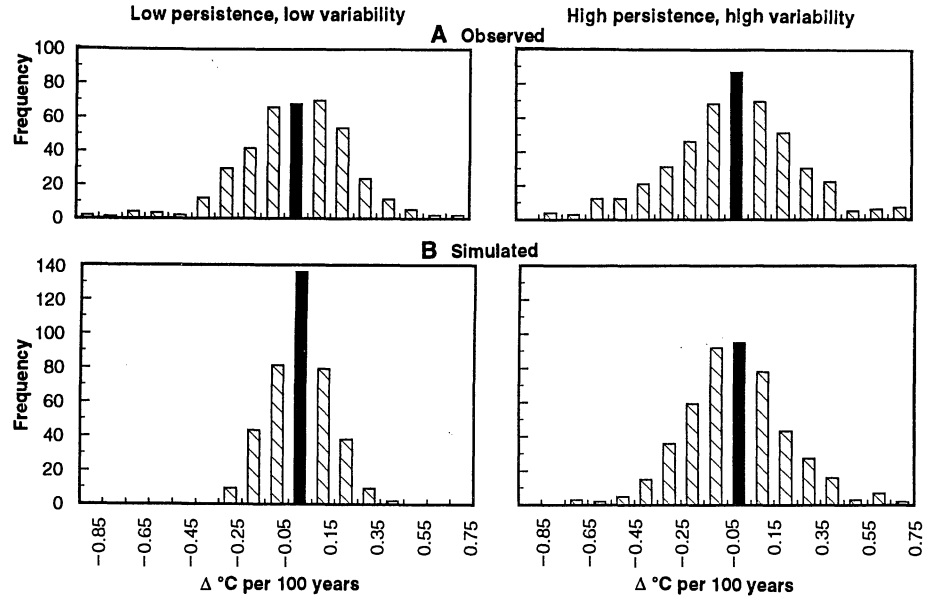

Fig. 1. Distribution of the observed differences (Δ°C per century) of monthly trends in mean daily minimum temperature between standard deseasonalized monthly anomalies and those calculated using a shifted calendar consistent with the Earth's precession of orbit (**A**) versus those simulated where only the effects of seasonality and day-to-day weather variability are active (**B**). Each set of differences is categorized by variance and day-to-day persistence of weather anomalies (both quantities are partitioned by the upper and lower one-half of the distribution of values for all months and all stations). Dark center, little or no difference; striped bars, positive or negative differences.